Supplementary Information (SI) for Journal of Materials Chemistry A.
This journal is © The Royal Society of Chemistry 2024

Supporting information for

Self-supported N-doped Carbon-coupled Ni-Co Binary Nanoparticles Electrodes Derived from Bionic Design of Wood Cell Wall for Durable Overall Water Splitting

Congcong Yang [#a], Ruixi Jin [#a], Zhihang Liu [a], Shilei Li [a], Dong Lv [a], Jingshuo Liu [a], Jian Li [a], Zhiqun Lin [*b], Likun Gao [*a]

a. Key Laboratory of Bio-based Material Science & Technology, Ministry of Education, Northeast Forestry University, Harbin 150040, PR China

b. Department of Chemical and Biomolecular Engineering, National University of Singapore, Singapore 117585

[#]These authors contributed equally: Congcong Yang and Ruixi Jin.

*Corresponding Authors: Likun Gao (gaolk@nefu.edu.cn) and Zhiqun Lin (z.lin@nus.edu.sg).

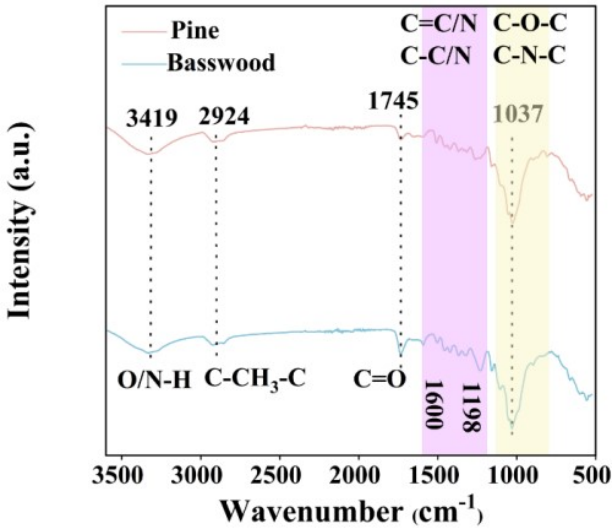

Fig. S1 FT-IR spectra of *Basswood* and *Pine*.

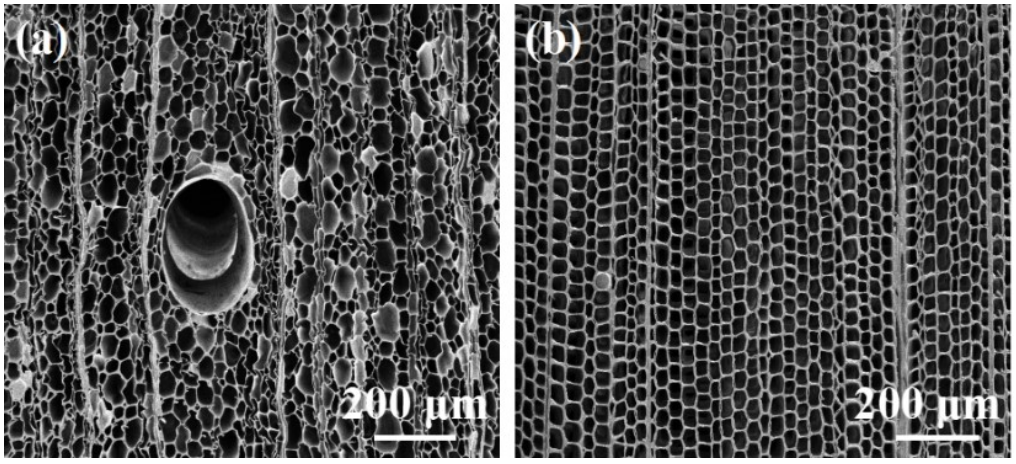

Fig. S2 SEM image of (a) untreated *Basswood* and (b) untreated *Pine* wood.

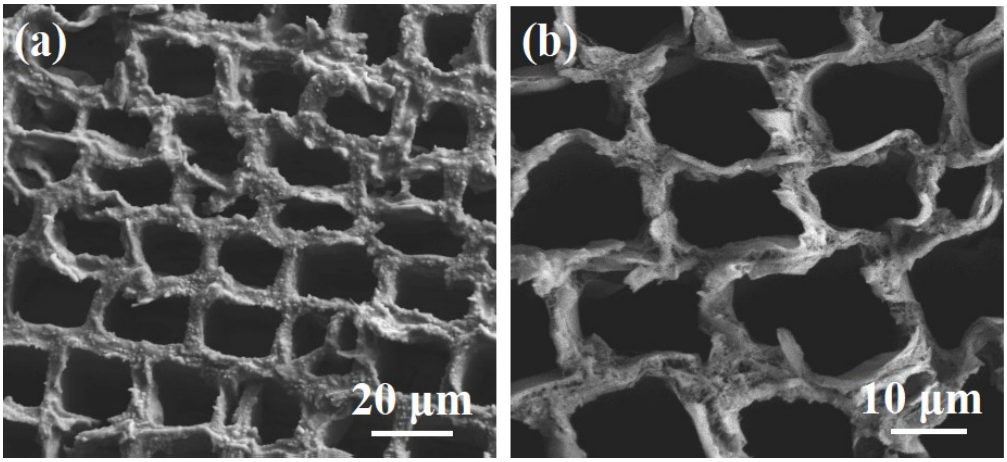

Fig. S3 SEM images of (a) *Pine* wood after treated with Co^{2+}, Ni^{2+} and polydopamine, and (b) Ni-Co/N@CW_P.

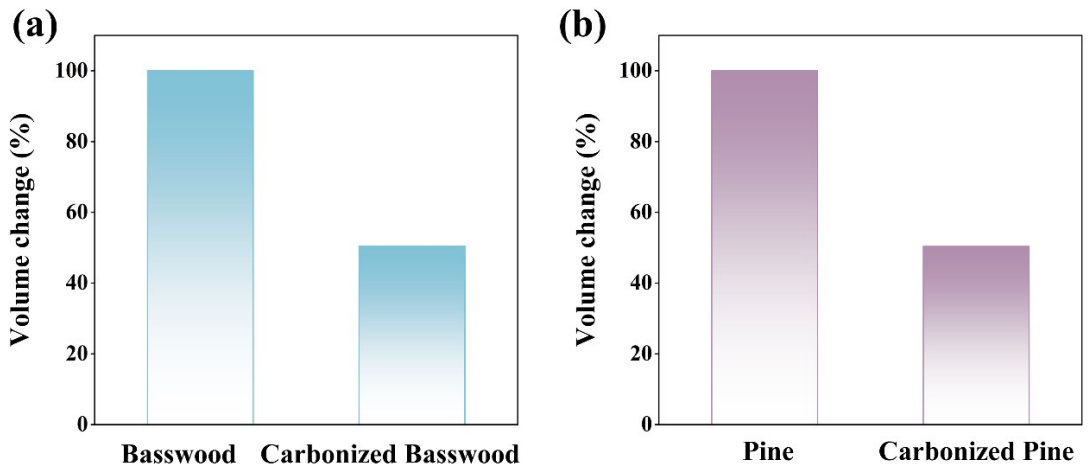

Fig. S4 The volume changes of (a) *Basswood* and (b) *Pine* before and after high-temperature calcination.

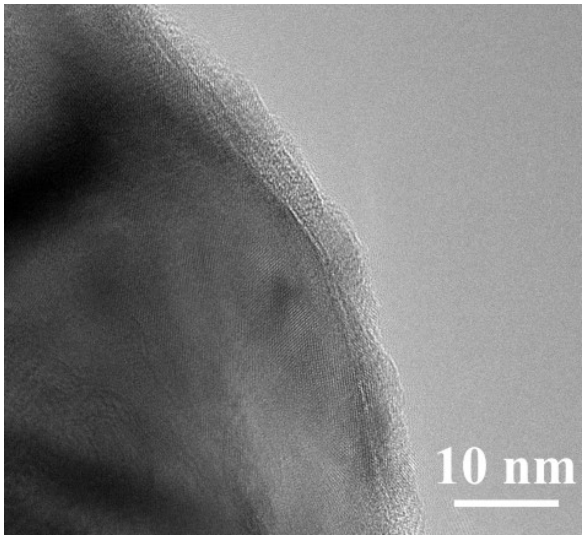

Fig. S5 High-resolution transmission electron microscope (HR-TEM) image of Ni-Co@CW_B.

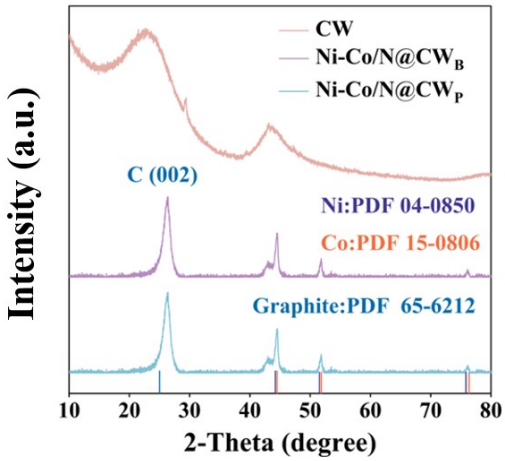

Fig. S6 XRD patterns of Ni-Co/N@CW$_B$, Ni-Co/N@CW$_P$, and carbonized wood.

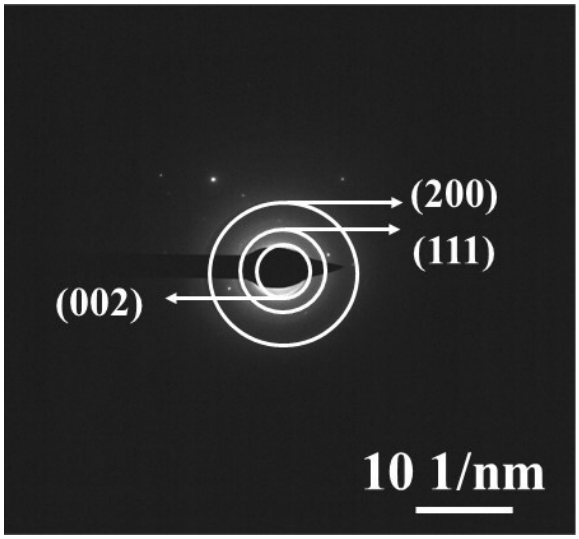

Fig. S7 The SAED pattern taken from the Ni-Co/N@CW_B.

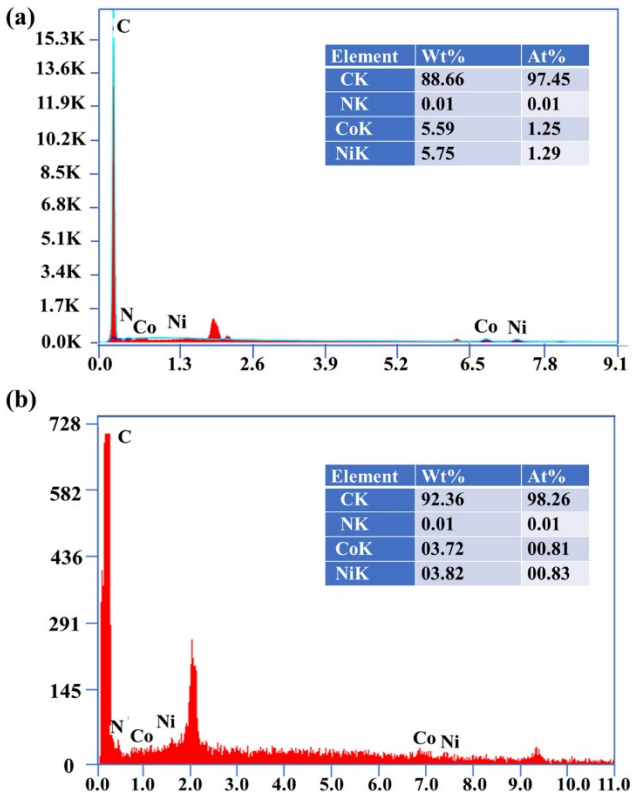

Fig. S8 EDX spectra of (a) Ni-Co/N@CW_B, and (b) Ni-Co/N@CW_P.

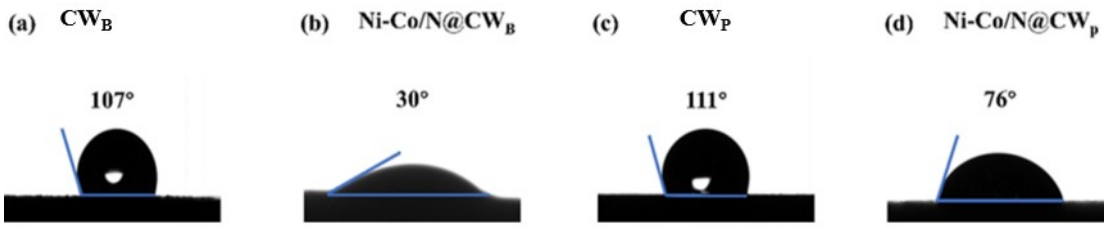

Fig. S9 Optical observation of contact angles of water droplets on the surfaces of (a) the CW_B, (b) Ni-Co/N@CW_B, (c) CW_P, and (d) Ni-Co/N@CW_P.

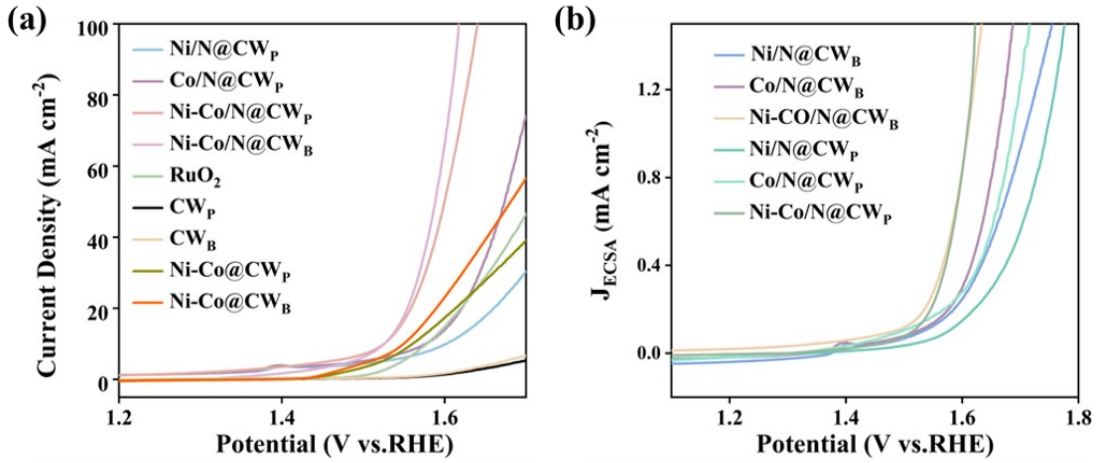

Fig. S10 (a) LSV curves for OER on CW_B, CW_P, Ni/N@CW_B, Ni/N@CW_P, Co/N@CW_B, Co/N@CW_P, Ni-Co@CW_B, Ni-Co@CW_P, Ni-Co/N@CW_B, Ni-Co/N@CW_P, and RuO_2. (b) LSV curves for OER on Ni/N@CW_B, Ni/N@CW_P, Co/N@CW_B, Co/N@CW_P, Ni-Co/N@CW_B, and Ni-Co/N@CW_P by normalizing to the ECSA.

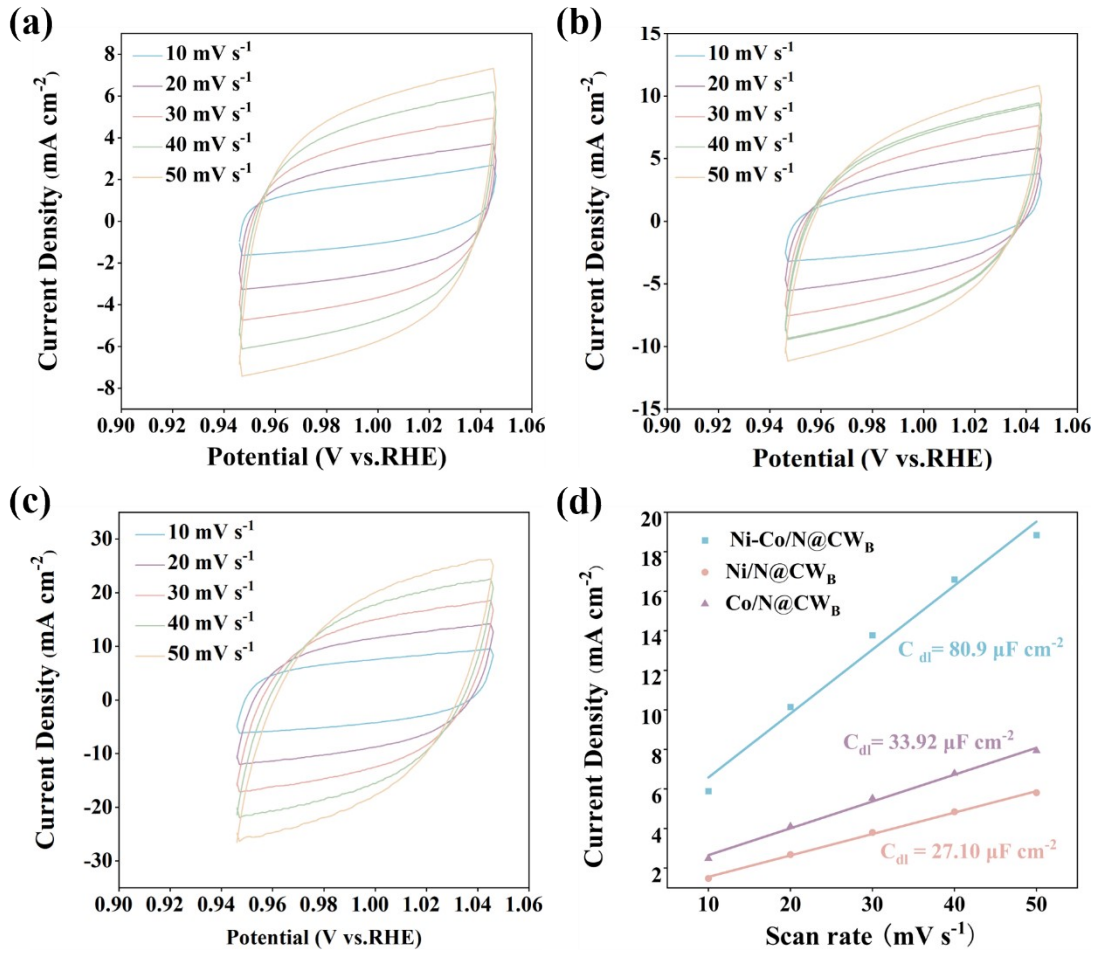

Fig. S11 Cyclic voltammetry (CV) curves measured at different scan rates from 10 to 50 m V s^{-1} for (a) Ni/N@CW_B, (b) Co/N@CW_B and (c) Ni-Co/N@CW_B. (d) The double-layer capacitance (C_{dl}) plots of Ni/N@CW_B, Co/N@CW_B and Ni-Co/N@CW_B.

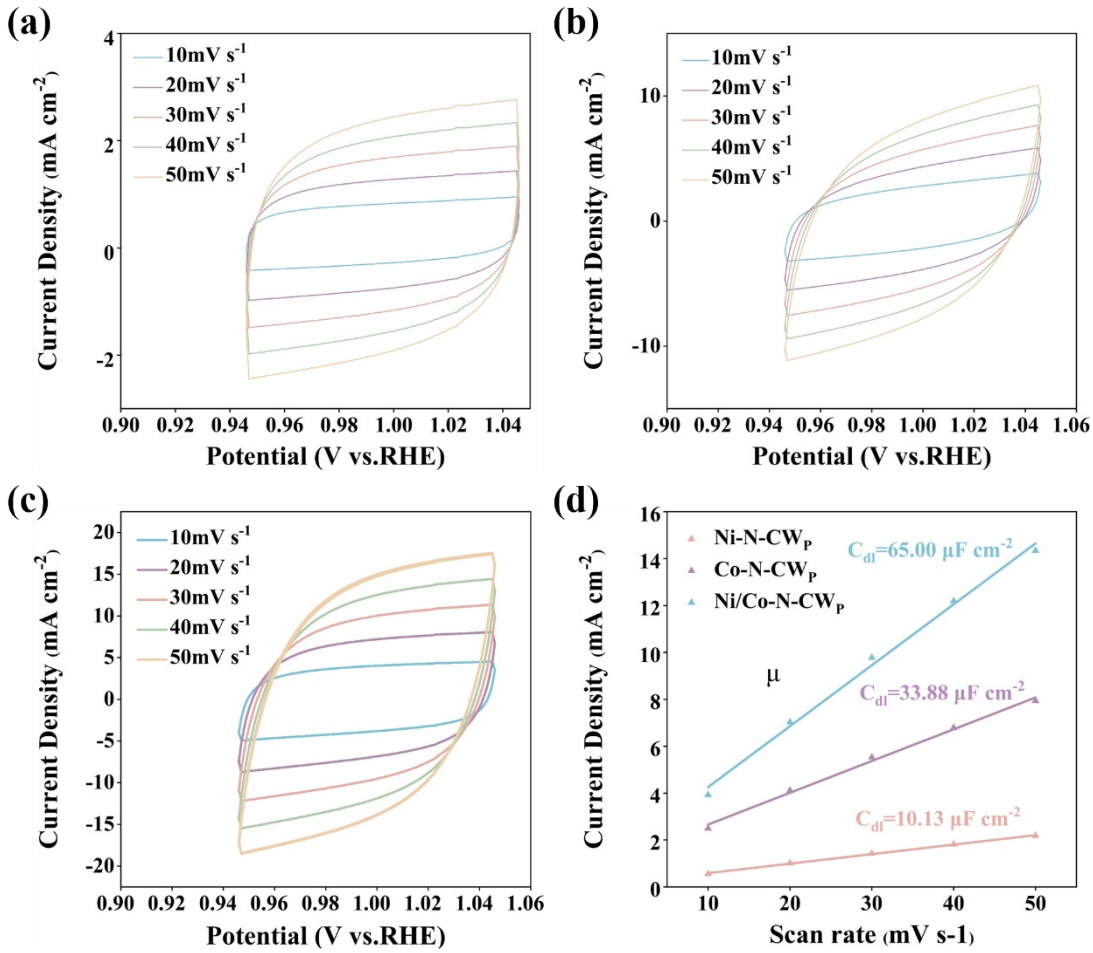

Fig. S12 Cyclic voltammetry (CV) curves measured at different scan rates from 10 to 50 m V s^{-1} for (a) Ni/N@CW_P, (b) Co/N@CW_P and (c) Ni-Co/N@CW_P. (d) The double-layer capacitance (C_{dl}) plots of Ni/N@CW_P, Co/N@CW_P, Ni-Co/N@CW_P.

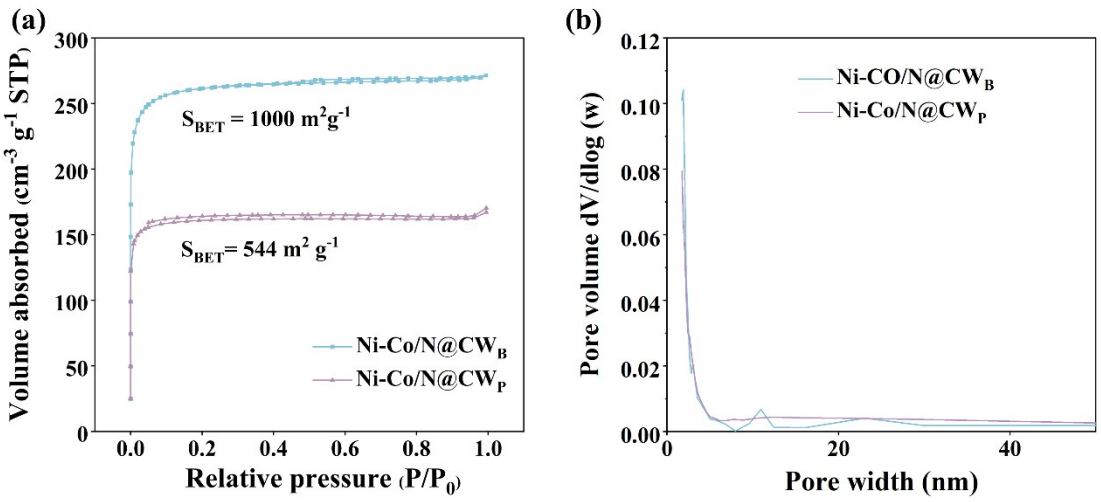

Fig. S13 (a) N_2 adsorption-desorption isotherms of Ni-Co/N@CW_B and Ni-Co/N@CW_P. (b) Pore size distribution curves of Ni-Co/N@CW_B and Ni-Co/N@CW_P.

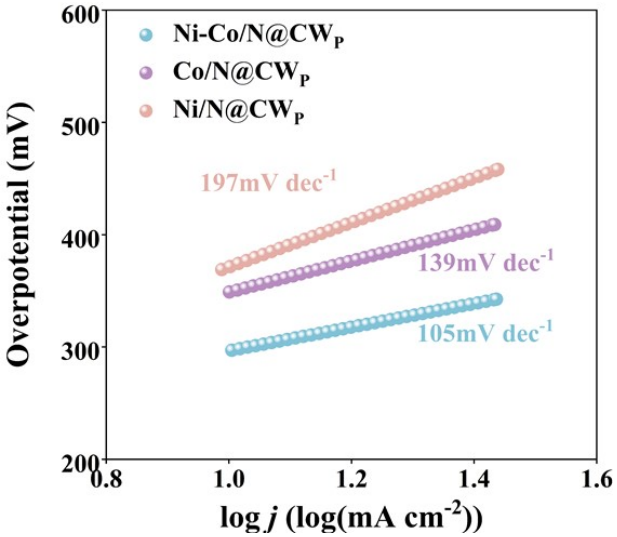

Fig. S14 Tafel plots for OER on Ni-Co/N@CW$_P$, Ni/N@CW$_P$, and Co/N@CW$_P$.

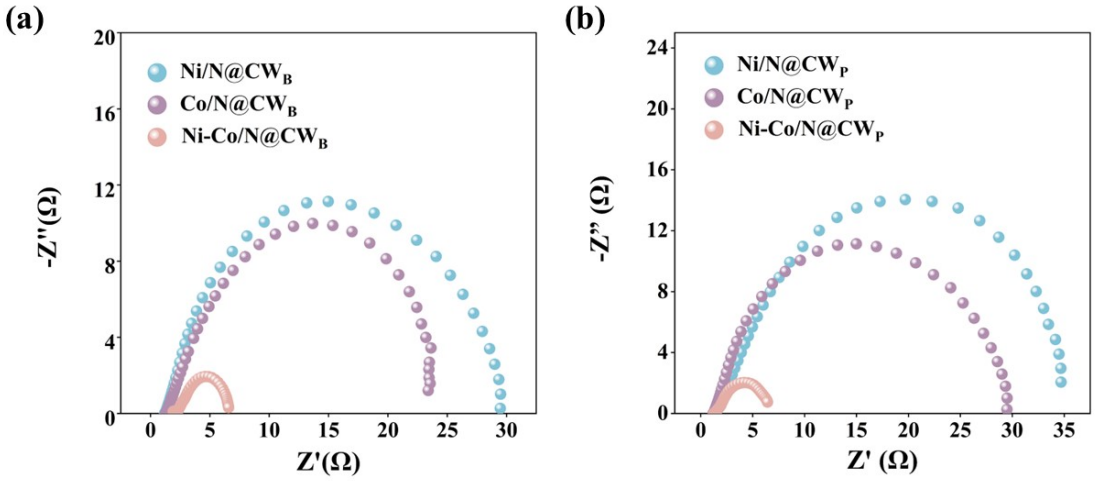

Fig. S15 (a) Nyquist plots of Ni/N@CW$_B$, Co/N@CW$_B$ and Ni-Co/N@CW$_B$. (b) Nyquist plots of Ni/N@CW$_P$, Co/N@CW$_P$ and Ni-Co/N@CW$_P$.

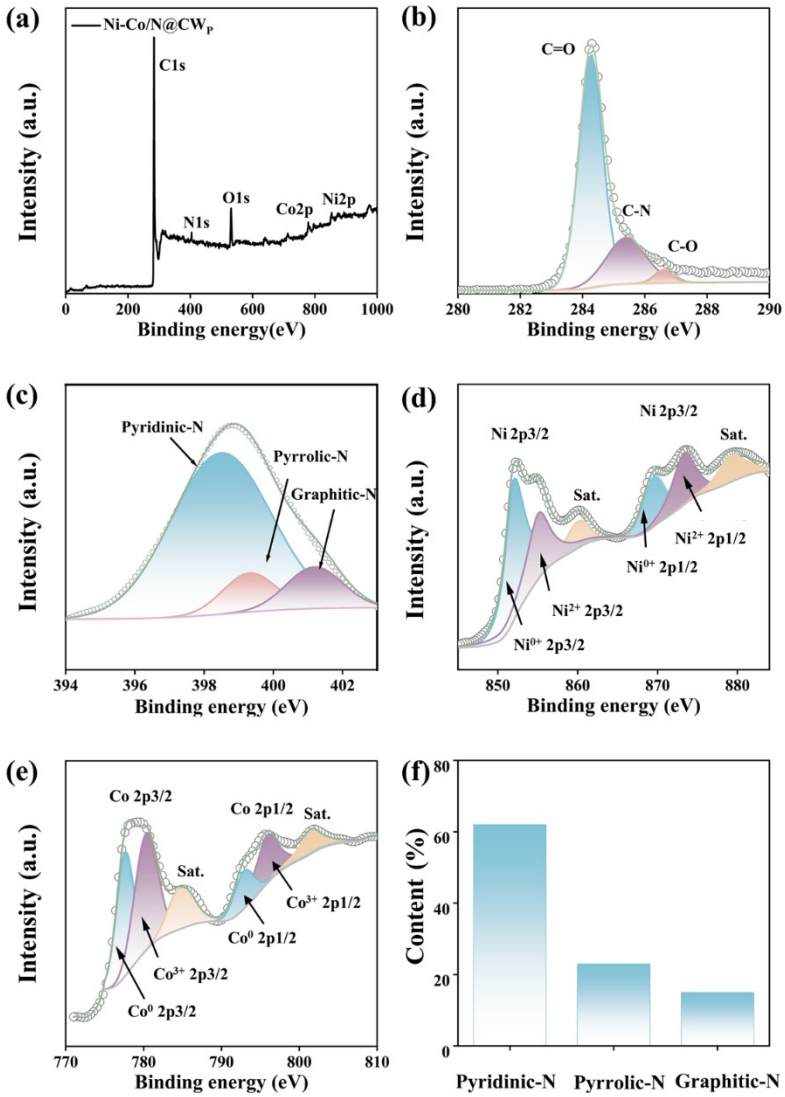

Fig. S16 (a) Survey XPS spectrum of Ni-Co/N@CW$_P$. (b) C 1s, (c) N 1s and (d) Ni 2p (e) Co 2p XPS spectra of Ni-Co/N@CW$_P$. (f) Percentages of N species obtained by N 1s spectra.

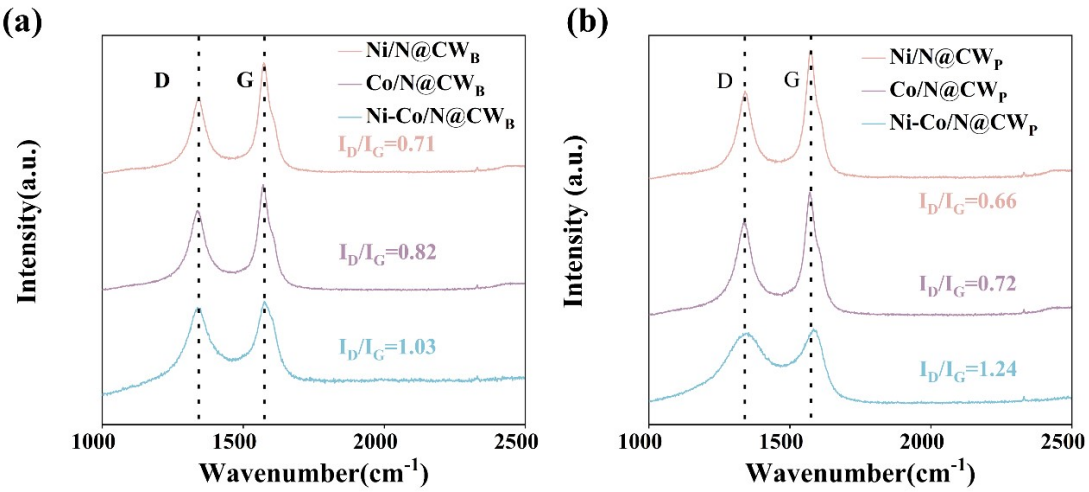

Fig. S17 (a) Raman spectra of Ni/N@CW$_B$, Co/N@CW$_B$ and Ni-Co/N@CW$_B$. (b) Raman spectra of Ni/N@CW$_P$, Co/N@CW$_P$ and Ni-Co/N@CW$_P$.

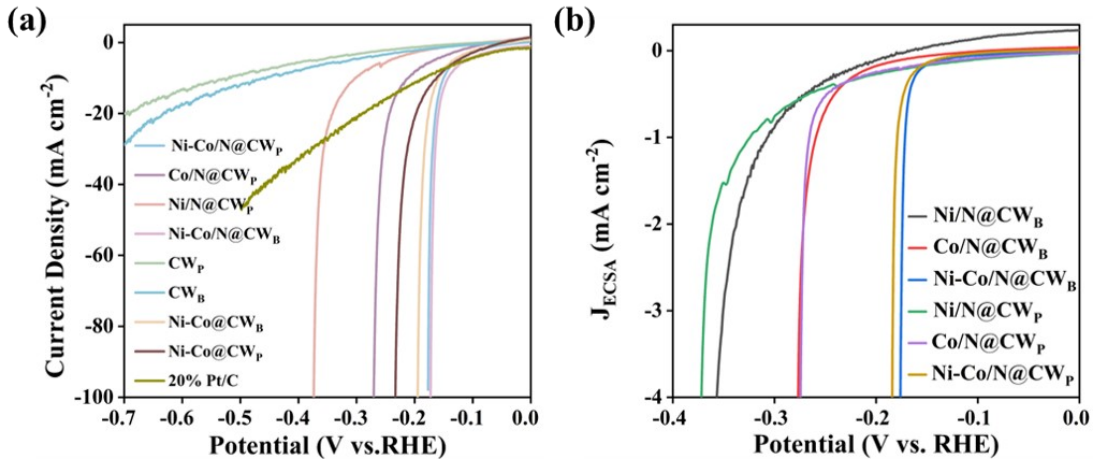

Fig. S18 (a) LSV curves for HER on CW_B, CW_P, $Ni/N@CW_B$, $Ni/N@CW_P$, $Co/N@CW_B$, $Co/N@CW_P$, $Ni\text{-}Co@CW_B$, $Ni\text{-}Co@CW@_P$, $Ni\text{-}Co/N@CW_B$, $Ni\text{-}Co/N@CW_P$, and Pt/C. (b) LSV curves for HER on $Ni/N@CW_B$, $Ni/N@CW_P$, $Co/N@CW_B$, $Co/N@CW_P$, $Ni\text{-}Co/N@CW_B$, and $Ni\text{-}Co/N@CW_P$ by normalizing to the ECSA.

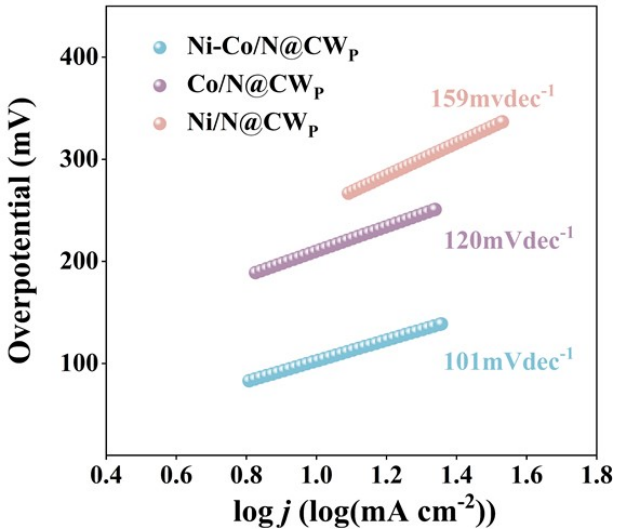

Fig. S19 Tafel plots for HER on Ni-Co/N@CW$_P$, Ni/N@CW$_P$ and Co/N@CW$_P$.

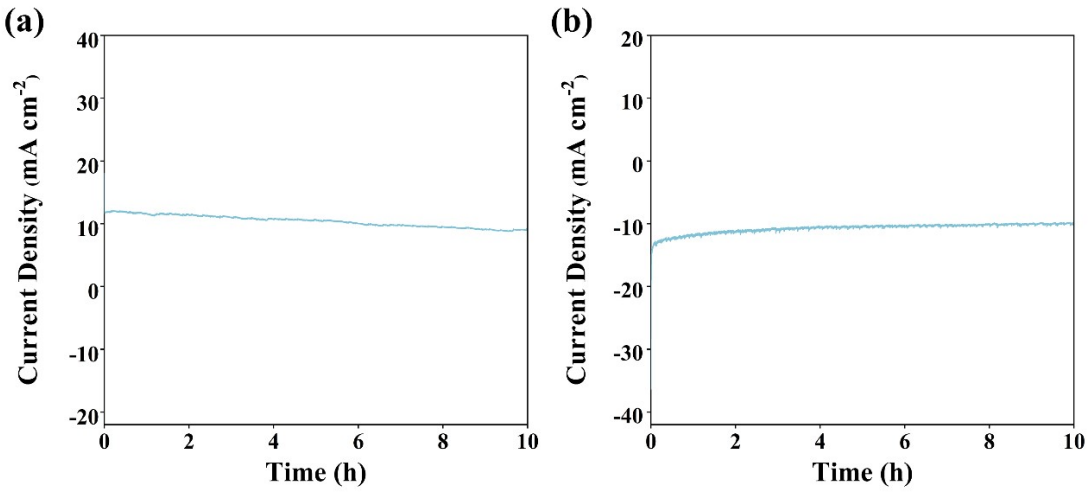

Fig. S20 Chronoamperometric responses for (a) OER and (b) HER of the Ni-Co/N@CW$_P$.

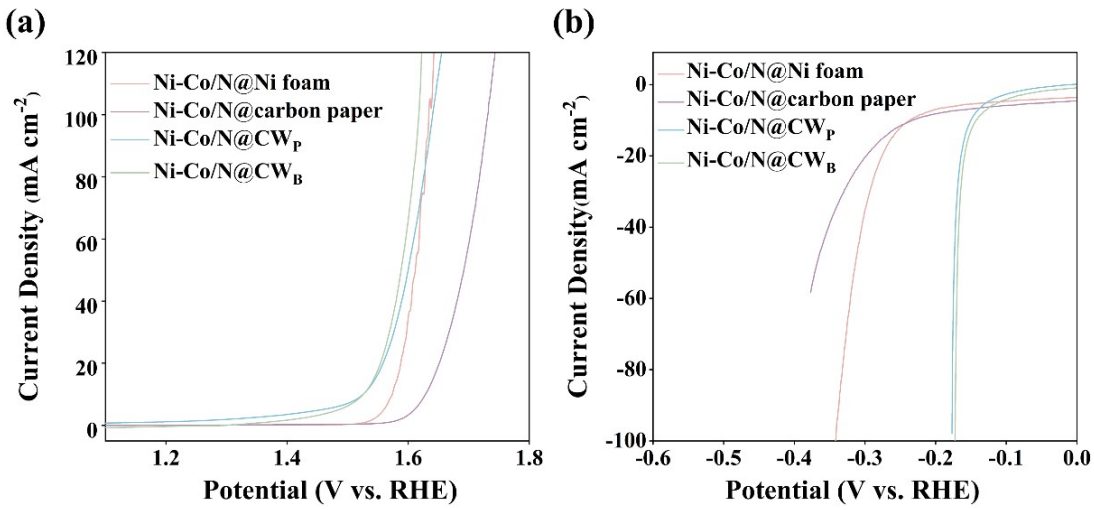

Fig. S21 (a) LSV curves for OER on Ni-Co/N@Ni foam, Ni-Co/N@carbon paper, Ni-Co/N@CW$_B$ and Ni-Co/N@CW$_P$, respectively. (b) LSV curves for HER on Ni-Co/N@Ni foam, Ni-Co/N@carbon paper, Ni-Co/N@CW$_B$ and Ni-Co/N@CW$_P$, respectively.

Table S1. The performance comparison of Ni-Co/N@CW with other reported works.

Electrocatalysts	Overpotential of HER @10 mA cm^{-2} (mV *vs.* RHE)	Overpotential of OER @10 mA cm^{-2} (mV *vs.* RHE)	Cell voltage @10mA cm^{-2} (V *vs.* RHE)	Electrolyte	Ref.
Ni-Co/N@CW_B	143	290	1.60	1.0 M KOH	This work
Ni-Co/N@CW_P	150	300	1.64	1.0 M KOH	This work
CoNiRu-NT	22	255	1.47	1.0 M KOH	1
Ru-CoV-LDH@NF	32	230	1.50	1.0 M KOH	2
Cu_3Ag_7/CF	130	289	1.99	1.0 M KOH	3
$MoS_2/NiCo_2O_4$/NF	322	106	1.62	1.0 M KOH	4
Ni/$Ni(OH)_2$	77	270	1.59	1.0 M KOH	5
Fe–Co–O/Co@NC-mNS/NF	112	257	1.58	1.0 M KOH	6
$Co_{0.42}Fe_{0.58}$P@C	178	226	1.55	1.0 M KOH	7
FeCoNiPtRu	104	331	1.69	1.0 M KOH	8
$CoPt_3$/a-FCWO-NS	135	243	1.51	1.0 M KOH	9
Co-Co_2C/CC	96	261	1.63	1.0 M KOH	10
Mn-NiCoP	148	266	1.62	1.0 M KOH	11
$NiP_2/NiSe_2$	89	250	1.56	1.0 M KOH	12

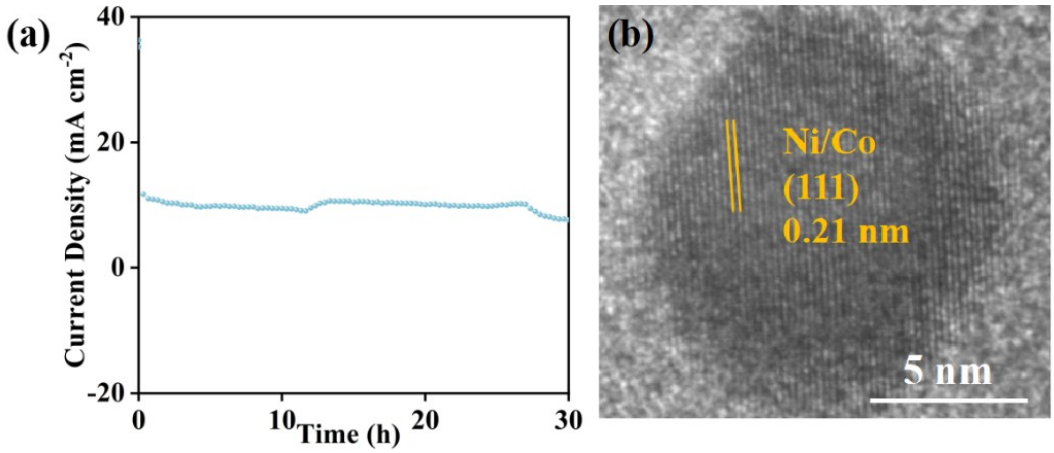

Fig. S22 (a) Chronoamperometric electrolysis in 1.0 M KOH at current density of 10 mA cm^{-2} for Ni-Co/N@CW_B || Ni-Co/N@CW_B over 30 h. (b) TEM image of Ni-Co/N@CW_B after water splitting stability test.

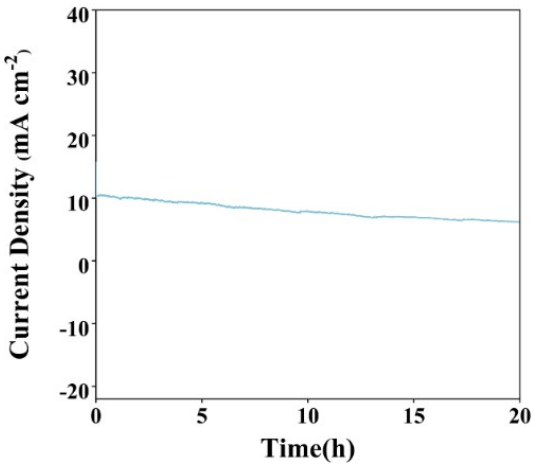

Fig. S23 Chronoamperometric electrolysis in 1.0 M KOH at current density of 10 mA cm^{-2} for Ni-Co/N@CW_P || Ni-Co/N@CW_P over 20 h.

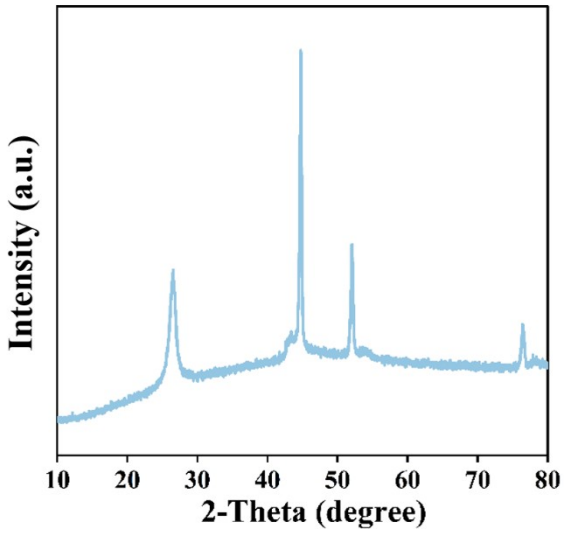

Fig. S24 XRD pattern of Ni-Co/N@CW after OER test.

Table S2. Weight % of metal loading obtained from ICP-OES analysis.

Sample	ICP-OES	
	Ni (*wt*%)	Co (*wt*%)
Post-reaction electrolyte (Ni-Co/N@CW_B)	0.02	0.03
Post-reaction electrolyte (Ni-Co/N@CW_P)	0.03	0.05

SI Refences

[1] W. Ying, W. Shuo, M. Z. Lin, Y. L. Ting, Z. X. Bo, X. Y. Ying, H. J. Min, Y. Xiao, L. S. Ni, Z. Q. Guo, Adv. Mater. 34 (2022) 2107488-2107501.

[2] L. Wei, F. Bomin, Y. Lingya, L. Junying, H. Weihua, ChemSusChem. 14 (2020) 730-737.

[3] K.N. Dinh, Y. Sun, Z. Pei, Z. Yuan, A. Suwardi, Q. Huang, X. Liao, Z. Wang, Y. Chen, Q. Yan, Small. 16 (2020) 1905885.

[4] M. Khairy, K.G. Mahmoud, J. Alloys. Compound. 935 (2023) 168056.

[5] T. Bairui, Y. Le, M. Fengjuan, Z. Yu, C. K. Paul, J. Phys. Chem.Solids. 150 (2021) 109842.

[6] T.I. Singh, G. Rajeshkhanna, U.N. Pan, T. Kshetri, H. Lin, N.H. Kim, J.H. Lee, Small. 17 (2021) 2101312.

[7] Y. Deng, Y. Cao, Y. Xia, X. Xi, Y. Wang, W. Jiang, D. Yang, A. Dong, T. Li, Adv. Energy Mater. 12 (2022) 2202394.

[8] H. Wu, Z. Wang, Z. Li, Y. Ma, F. Ding, F. Li, H. Bian, Q. Zhai, Y. Ren, Y. Shi, Adv. Energy Mater. 13 (2023) 2300837.

[9] Z. Wang, S. Li, G. Zhang, X. Yu, Z. Zhao, Y. Zhang, Y. Shi, H.-B. Zhu, X. Xiao, Appl. Catal. B Environ. 342 (2024) 123387.

[10] P. Wang, J. Zhu, Z. Pu, R. Qin, C. Zhang, D. Chen, Q. Liu, D. Wu, W. Li, S. Liu, Appl. Catal. B Environ. 296 (2021) 120334

[11] G. Ma, J. Ye, M. Qin, T. Sun, W. Tan, Z. Fan, L. Huang, X. Xin, Nano Energy. 115 (2023) 108679.

[12] L. Yang, L. Huang, Y. Yao, L. Jiao, Appl. Catal. B Environ. 282 (2021) 119584.